ELSEVIER

International Journal of Solids and Structures 41 (2004) 4279–4297

INTERNATIONAL JOURNAL OF SOLIDS and STRUCTURES

www.elsevier.com/locate/ijsolstr

Plastic buckling of rectangular plates subjected to intermediate and end inplane loads

C.M. Wang [a,*], Y. Chen [a], Y. Xiang [b]

[a] *Department of Civil Engineering, National University of Singapore, Kent Ridge, Singapore 119260, Singapore*
[b] *School of Engineering and Industrial Design & Centre for Construction Technology and Research, University of Western Sydney, Locked Bag 1797, Penrith South DC, NSW 1797, Australia*

Received 21 February 2004; received in revised form 21 February 2004
Available online 10 April 2004

Abstract

This paper is concerned with the plastic buckling of rectangular plates subjected to both intermediate and end uniaxial loads. The plate has two opposite simply supported edges that are parallel to the load direction while the other remaining edges may take any combination of free, simply supported or clamped conditions. Both the incremental theory of plasticity and the deformation theory of plasticity are considered in bounding the plastic behaviour of the plate. The buckling problem is solved by decomposing the plate into two sub-plates at the boundary where the intermediate load acts. Each sub-plate buckling problem is solved exactly using the Levy approach and the two solutions brought together by the continuity equations at the separated interface. There are eight possible solutions for each sub-plate and consequently there are 64 combinations of solutions to be considered for the entire plate. The final solution combination depends on the nature of the ratio of the intermediate load to the end load, the intermediate load location, aspect ratio, and material properties. Typical plastic stability criteria are presented in graphical forms which should be useful for engineers designing plated walls that support intermediate floors/loads.

Keywords: Plastic buckling; Rectangular plates; Intermediate load; Levy method; Stability criteria; Incremental theory of plasticity; Deformation theory of plasticity

1. Introduction

The elastic buckling problem of rectangular plates under uniaxial loads acting at opposite ends is the most basic plate buckling problem and its solution is documented in most standard texts on plate buckling (for example Timoshenko and Gere, 1961; Bulson, 1970). Recently, Wang et al. (2004) extended this buckling problem to include an intermediate uniaxial load in addition to the end uniaxial loads as shown in Fig. 1. This problem has practical applications in vertical plate structures/walls that are required to carry an

* Corresponding author. Tel.: +65-6874-2157; fax: +65-6779-1635.
E-mail address: cvewcm@nus.edu.sg (C.M. Wang).

0020-7683/$ - see front matter © 2004 Elsevier Ltd. All rights reserved.
doi:10.1016/j.ijsolstr.2004.02.051

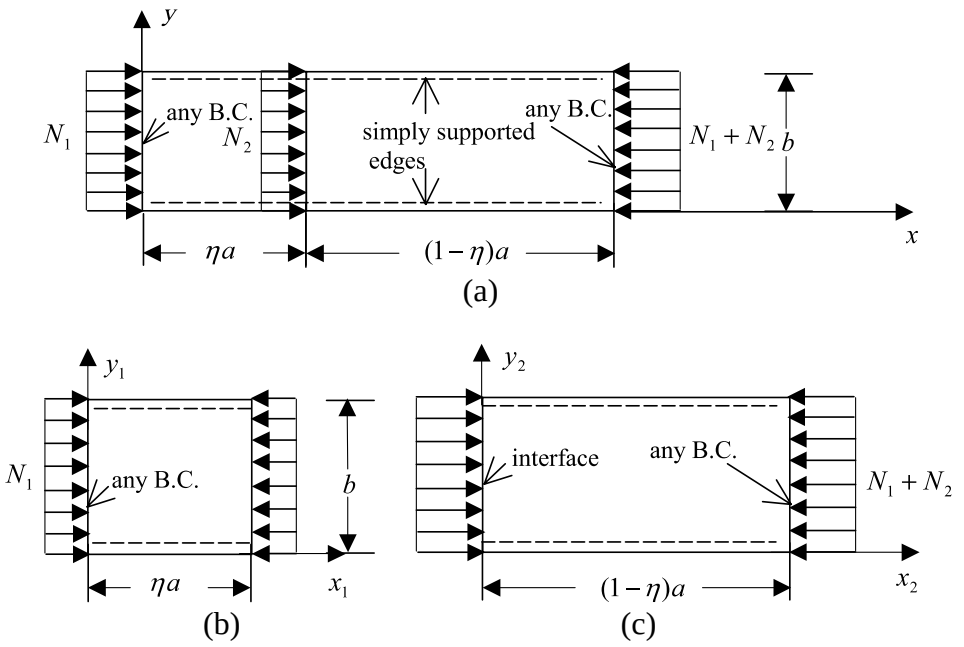

Fig. 1. Rectangular plate under intermediate and end uniaxial loads.

intermediate floor. Wang et al. (2004) solved this problem by decomposing the plate into two sub-plates at the boundary where the intermediate load acts. Each sub-plate buckling problem is solved exactly using the Levy approach and the two solutions brought together by the continuity equations at the interfacial edge. This elastic plate buckling problem has five possible solutions for each sub-plate and consequently there are 25 solution combinations to be considered. The final solution combination depends on the aspect ratio and the intermediate to end load ratios.

This paper continues in this line of investigation by considering the plastic buckling behavior of the plate. In order to bound the plastic behaviour, we shall use two competing theories of plasticity, namely, the incremental theory of plasticity (IT) and the deformation theory of plasticity (DT). IT was proposed by Prager (1938, 1941, 1942a,b), Handelman and Prager (1948) and Sewell (1963) while DT was advanced by Hencky (1925), Nadai (1944), Ilyushin (1946), Shanley (1946), Stowell (1948) and Bijlaard (1949). The two theories may yield somewhat different buckling load values with DT predicting smaller buckling loads than those obtained by IT. It is interesting to note that despite the physical shortcoming of DT, the buckling loads predicted have been found to be in better agreement with test results than that furnished by the more physically realistic IT (Pride and Heimerl, 1949; Hutchinson, 1974; El-Ghazaly and Sherbourne, 1986; Durban, 1998). This unexpected buckling behaviour could be due to geometrical and other irregularities not considered in the theoretical treatment (Chakrabarty, 2002).

The rectangular plate considered herein has two opposite edges simply supported and parallel to the direction of the applied uniaxial loads while the other two plate edges can take any combination of free, simply supported or clamped conditions. The uniaxial loads act at the ends of the plate as well as at an intermediate location in the plate domain. The aim of this paper is to derive analytical plastic buckling solutions for such loaded plates. These analytical solutions elucidate the intrinsic, fundamental and unexpected features of the solutions. Moreover the exact buckling solutions serve as useful benchmark values for researchers developing numerical methods for plastic buckling analysis of plates and shells. First, however, a brief review of the recent literature (from 1995 onwards) in this field is given.

Durban and Zuckerman (1999) carried out a detailed parametric study on the elasto-plastic buckling of rectangular plates under biaxial compression. Apart from confirming that DT furnishes lower buckling stresses than those computed using IT, they reported the existence of an optimal loading part for DT model. Betten and Shin (2000) investigated the influences of aspect ratios, load ratios and hardening factors on the buckling stresses of rectangular plates subjected to biaxial loads. Moen et al. (1998) studied the effect of plastic anisotropy on the elasto-plastic buckling behaviour of anisotropic aluminum plate elements. Soh et al. (2000) studied the plastic buckling of a simply supported, rectangular, composite plate subjected to edge compression. The fibre composite plates considered include carbon epoxy, glass epoxy and boron aluminum plates. Their theoretical results obtained are deemed comparable to experimental test results. Chakrabarty (2002) demonstrated the influence of plastic anisotropy on the buckling stress for the plastic buckling of rectangular plates under unidirectional compression. The buckling stress is shown to be significantly lowered by the presence of plastic anisotropy when compared to the corresponding isotropic material.

The subject on plastic buckling of thick plates was relatively less studied by researchers. One of the early papers on plastic buckling of thick plates is by Shrivastava (1979, 1995). He derived closed form expressions for the buckling loads of (a) infinitely long simply supported plates, (b) simply supported square plates and (c) infinitely long plates that are simply supported on three sides and free on one unloaded edge. Wang et al. (2001) derived analytically the elastic/plastic stability criteria for (a) uniaxially and equibiaxially loaded rectangular plates with two opposite edges simply supported while the other two edges may take on any combination of free, simply supported or clamped boundary condition and (b) uniformly inplane loaded circular plates with either simply supported edge or clamped edge. Wang (2004) treated the plastic buckling of uniformly inplane loaded, simply supported, polygonal, thick plates and gave an analytical relationship between the plastic buckling load and its corresponding elastic thin plate buckling load.

2. Mathematical modeling

2.1. Problem definition

Consider an isotropic, rectangular thin plate as shown in Fig. 1a. The plate has length a, width b, and thickness h and is simply supported along the edges $y = 0$ and $y = b$. The other two edges of the plate may take any combination of free (F), simply supported (S) and clamped (C) conditions. For convenience, a four-letter symbol is used to denote the support conditions of the plate. For example, an FSCS plate has a free left edge, a simply supported bottom edge, a clamped right edge and a simply supported top edge.

The plate is subjected to an end load $N_1 = \sigma_1 h$ (per unit length) at the edge $x = 0$ and an intermediate load $N_2 = \sigma_2 h$ (per unit length) at the location $x = \eta a$. Thus the end reaction force at the right edge $x = a$ is $N_1 + N_2 = (\sigma_1 + \sigma_2)h$ as shown in Fig. 1. A positive value of σ implies a compressive load while a negative value implies a tensile uniaxial load. The material of the plate is assumed to obey the Ramberg–Osgood constitutive law. The problem at hand is to determine the plastic buckling load for such a loaded plate.

2.2. Method of solution

The plate is first divided into two sub-plates. The first sub-plate is to the left of the vertical line defined by $x = \eta a$ (see Fig. 1b) and the second sub-plate is to the right of this line (see Fig. 1c). Adopting the x–y coordinate systems as shown in Fig. 1b and c, the governing plastic buckling equation for each sub-plate may be canonically written as (see Chakrabarty, 2000)

$$\alpha\frac{\partial^4 w}{\partial x^4}+2\beta\frac{\partial^4 w}{\partial x^2\partial y^2}+\gamma\frac{\partial^4 w}{\partial y^4}=-\frac{12}{h^2}\frac{\sigma}{E}\frac{\partial^2 w}{\partial x^2} \tag{1}$$

in which w is the transverse displacement at the midplane of the plate, σ the inplane stress of the sub-plate, and the parameters α, β, γ, μ are defined as follows:

- *Based on incremental theory of plasticity (IT)*:

$$\alpha=\frac{1}{\rho}\left[1+3\frac{T}{E}\right],\qquad \beta=\frac{1}{\rho}\left[2-2(1-2v)\frac{T}{E}\right]+\frac{1}{1+v}, \tag{2a,b}$$

$$\gamma=\frac{4}{\rho},\qquad \rho=(5-4v)-(1-2v)^2\frac{T}{E}. \tag{2c,d}$$

- *Based on deformation theory of plasticity (DT)*:

$$\alpha=\frac{1}{\rho}\left[1+3\frac{T}{S}\right],\qquad \beta=\frac{1}{\rho}\left[2-2(1-2v)\frac{T}{E}\right]+\frac{1}{1+v}, \tag{3a,b}$$

$$\gamma=\frac{4}{\rho},\qquad \rho=3\frac{E}{S}+(1-2v)\left[2-(1-2v)\frac{T}{E}\right], \tag{3c,d}$$

where v is the Poisson ratio, and the ratios of the elastic modulus E to the tangential modulus T and the secant modulus S at the onset of buckling are expressed as

$$\frac{E}{T}=1+ck\left(\frac{\sigma}{\sigma_0}\right)^{c-1},\quad c>1, \tag{4a}$$

$$\frac{E}{S}=1+k\left(\frac{\sigma}{\sigma_0}\right)^{c-1},\quad c>1, \tag{4b}$$

where σ_0 is a nominal yield stress, c the hardening index that describes the shape of the stress–strain relationship with $c=\infty$ for elastic-perfectly plastic response, and k the horizontal distance between the knee of $c=\infty$ and the intersection of the c curve with the $\sigma/\sigma_0=1$ line as shown in Fig. 2.

Let

$$\bar{w}_i=\frac{w_i}{b},\qquad \bar{x}_i=\frac{x_i}{a_i},\qquad \bar{y}_i=\frac{y_i}{b}, \tag{5a–c}$$

where $i=1,2$ respectively denotes the sub-plates 1 and 2; $a_1=\eta a$ and $a_2=(1-\eta)a$. In view of Eq. (5a)–(5c), Eq. (1) may be rewritten as

$$\alpha_i\frac{\partial^4\bar{w}_i}{\partial\bar{x}_i^4}+\frac{2\beta_i a_i^2}{b^2}\frac{\partial^4\bar{w}_i}{\partial\bar{x}_i^2\partial\bar{y}_i^2}+\frac{a_i^4\gamma}{b^4}\frac{\partial^4\bar{w}_i}{\partial\bar{y}_i^4}=-\frac{12\sigma_i a_i^2}{Eh^2}\frac{\partial^2\bar{w}_i}{\partial\bar{x}_i^2}. \tag{6}$$

Based on the Levy approach (Timoshenko and Woinowsky-Krieger, 1959), the solution to the partial differential equation may take the form of

$$\bar{w}_i(\bar{x}_i,\bar{y}_i)=A_{im}(\bar{x}_i)\sin m\pi\bar{y}_i,\quad i=1,2, \tag{7}$$

where m $(=1,2,\ldots,\infty)$ is the number of the half waves of the buckling mode in the y-direction. In view of Eq. (7), the partial differential equation (6) may be reduced into an ordinary differential equation given by

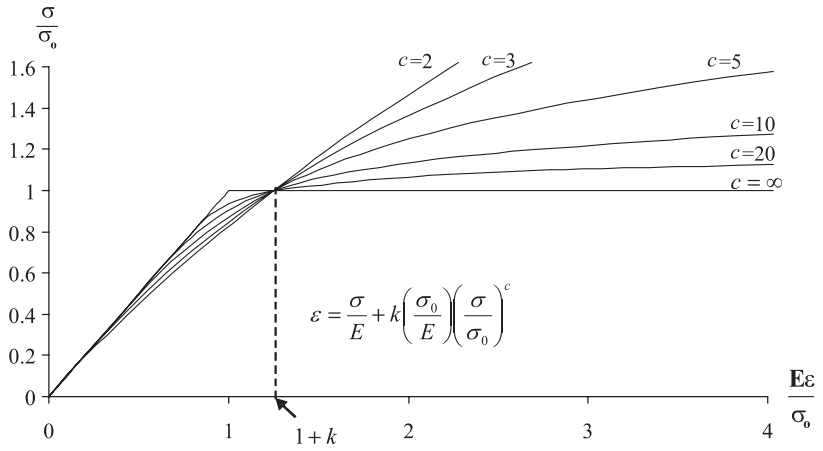

Fig. 2. Ramberg–Osgood stress–strain relation.

$$\frac{\mathrm{d}^4 A_{im}}{\mathrm{d}\bar{x}_i^4} + \left(\frac{12\sigma_i a_i^2}{Eh^2\alpha_i} - \frac{2\beta_i m^2\pi^2 a_i^2}{b^2\alpha_i}\right)\frac{\mathrm{d}^2 A_{im}}{\mathrm{d}\bar{x}_i^2} + \frac{a_i^4 m^4\pi^4\gamma_i}{b^4\alpha_i} = 0. \tag{8}$$

Three parameters Δ_1, Δ_2, and Δ_3 are defined as follows:

$$\Delta_1 = \left(\frac{12\sigma_i a_i^2}{Eh^2\alpha_i} - \frac{2\beta_i m^2\pi^2 a_i^2}{b^2\alpha_i}\right)^2 - \frac{4a_i^4 m^4\pi^4\gamma_i}{b^4\alpha_i}, \tag{9}$$

$$\Delta_2 = \frac{a_i^4 m^4\pi^4\gamma_i}{b^4\alpha_i}, \tag{10}$$

$$\Delta_3 = \frac{12\sigma_i a_i^2}{Eh^2\alpha_i} - \frac{2\beta_i m^2\pi^2 a_i^2}{b^2\alpha_i}. \tag{11}$$

Depending on the values of Δ_1, Δ_2 and Δ_3, there are eight possible solutions for the fourth-order differential equation (8). These solutions, designated as Solutions A–H, are given in Table 1.

Table 1
Types of solutions depending on values of Δ_1, Δ_2, Δ_3

Δ_1	Δ_2	Δ_3	Solution
>0	>0	>0	A
		<0	B
	=0	>0	C
		<0	D
	<0	Any value	E
=0	$=\frac{\Delta_3^2}{4}$	>0	F
		<0	G
<0	Any value	Any value	H

Solution A:

$$A_{im} = C_{i1}\cos\phi_i\bar{x}_i + C_{i2}\sin\phi_i\bar{x}_i + C_{i3}\cos\xi_i\bar{x}_i + C_{i4}\sin\xi_i\bar{x}_i \quad \text{in which } \phi_i = \sqrt{\frac{\Delta_3+\sqrt{\Delta_1}}{2}},$$

$$\xi_i = \sqrt{\frac{\Delta_3-\sqrt{\Delta_1}}{2}}. \tag{12}$$

Solution B:

$$A_{im} = C_{i1}\cosh\phi_i\bar{x}_i + C_{i2}\sinh\phi_i\bar{x}_i + C_{i3}\cosh\xi_i\bar{x}_i + C_{i4}\sinh\xi_i\bar{x}_i \quad \text{in which } \phi_i = \sqrt{\frac{-\Delta_3+\sqrt{\Delta_1}}{2}},$$

$$\xi_i = \sqrt{\frac{-\Delta_3-\sqrt{\Delta_1}}{2}}. \tag{13}$$

Solution C:

$$A_{im} = C_{i1}\cos\phi_i\bar{x}_i + C_{i2}\sin\phi_i\bar{x}_i + C_{i3}\bar{x}_i + C_{i4} \quad \text{in which } \phi_i = \sqrt{\Delta_3}. \tag{14}$$

Solution D:

$$A_{im} = C_{i1}\cosh\phi_i\bar{x}_i + C_{i2}\sinh\phi_i\bar{x}_i + C_{i3}\bar{x}_i + C_{i4} \quad \text{in which } \phi_i = \sqrt{-\Delta_3}. \tag{15}$$

Solution E:

$$A_{im} = C_{i1}\cosh\phi_i\bar{x}_i + C_{i2}\sinh\phi_i\bar{x}_i + C_{i3}\cos\xi_i\bar{x}_i + C_{i4}\sin\xi_i\bar{x}_i \quad \text{in which } \phi_i = \sqrt{\frac{-\Delta_3+\sqrt{\Delta_1}}{2}},$$

$$\xi_i = \sqrt{\frac{\Delta_3+\sqrt{\Delta_1}}{2}}. \tag{16}$$

Solution F:

$$A_{im} = C_{i1}\cos\phi_i\bar{x}_i + C_{i2}\bar{x}_i\cos\phi_i\bar{x}_i + C_{i3}\sin\phi_i\bar{x}_i + C_{i4}\bar{x}_i\sin\phi_i\bar{x}_i \quad \text{in which } \phi_i = \sqrt{\frac{\Delta_3}{2}}. \tag{17}$$

Solution G:

$$A_{im} = C_{i1}\cosh\phi_i\bar{x}_i + C_{i2}\bar{x}_i\cosh\phi_i\bar{x}_i + C_{i3}\sinh\phi_i\bar{x}_i + C_{i4}\bar{x}_i\sinh\phi_i\bar{x}_i \quad \text{in which } \phi_i = \sqrt{\frac{-\Delta_3}{2}}. \tag{18}$$

Solution H:

$$A_{im} = C_{i1}\cosh\phi_i\bar{x}_i\cos\xi_i\bar{x}_i + C_{i2}\cosh\phi_i\bar{x}_i\sin\xi_i\bar{x}_i + C_{i3}\sinh\phi_i\bar{x}_i\cos\xi_i\bar{x}_i + C_{i4}\sinh\phi_i\bar{x}_i\sin\xi_i\bar{x}_i$$

$$\text{in which } \phi_i = \frac{1}{2}\sqrt{-\Delta_3+\sqrt{\Delta_3^2-\Delta_1}}, \qquad \xi_i = \frac{1}{2}\sqrt{\Delta_3+\sqrt{\Delta_3^2-\Delta_1}}. \tag{19}$$

Note that the solutions of Eq. (8) that are given explicitly in Eqs. (12)–(19) involve real values only, i.e. ϕ_i and ξ_i are real values. We may employ the state-space technique to obtain the solutions for Eq. (8) as illustrated by Xiang et al. (2003). The solutions of Eq. (8) can also be expressed in a more compact form as shown by Ore and Durban (1992) if the complex roots of the characteristic equation of Eq. (8) are used in the solutions. One of the main reasons that prompted the authors to choose the current form of solutions for Eq. (8) is to reveal the buckling modes of the plates in an explicit form which is readily comprehended.

The eight real constants C_{1i}, C_{2i}, $i = 1,2,3,4$ resulting from the solution combination can be evaluated using the boundary equations at the edges $\bar{x}_1 = 0$ and $\bar{x}_2 = 1$.

- For simply supported edges:

$$\bar{w}_i = 0 \Rightarrow A_{im} = 0 \tag{20a}$$

and

$$\frac{\alpha_i}{a_i^2}\frac{\partial^2 \bar{w}_i}{\partial \bar{x}_i^2} + \frac{\beta_i - \mu}{b^2}\frac{\partial^2 \bar{w}_i}{\partial \bar{y}_i^2} = 0 \Rightarrow \frac{\alpha_i}{a_i^2}\frac{\mathrm{d}^2 A_{im}}{\mathrm{d}\bar{x}_i^2} - \frac{(\beta_i - \mu)m^2\pi^2}{b^2}A_{im} = 0, \quad i = 1,2, \tag{20b}$$

where $\mu = 1/(1+\nu)$.

- For clamped edges:

$$\bar{w}_i = 0 \Rightarrow A_{im} = 0 \tag{21a}$$

and

$$\frac{\partial \bar{w}_i}{\partial \bar{x}_i} = 0 \Rightarrow \frac{\mathrm{d}A_{im}}{\mathrm{d}\bar{x}_i} = 0, \quad i = 1,2. \tag{21b}$$

- For free edges:

$$\frac{\alpha_i}{a_i^2}\frac{\partial^2 \bar{w}_i}{\partial \bar{x}_i^2} + \frac{\beta_i - \mu}{b^2}\frac{\partial^2 \bar{w}_i}{\partial \bar{y}_i^2} = 0 \Rightarrow \frac{\alpha_i}{a_i^2}\frac{\mathrm{d}^2 A_{im}}{\mathrm{d}\bar{x}_i^2} - \frac{(\beta_i - \mu)m^2\pi^2}{b^2}A_{im} = 0 \tag{22a}$$

and

$$\frac{\alpha_i}{a_i^3}\frac{\partial^3 \bar{w}_i}{\partial \bar{x}_i^3} + \frac{\beta_i + \mu}{a_i b^2}\frac{\partial^3 \bar{w}_i}{\partial \bar{x}_i \partial \bar{y}_i^2} + \frac{12\sigma_i b}{Eh^2 a_i}\frac{\partial \bar{w}_i}{\partial \bar{x}_i} = 0 \Rightarrow \frac{\alpha_i}{a_i^3}\frac{\mathrm{d}^3 A_{im}}{\partial \bar{x}_i^3} + \left(\frac{12\sigma_i b}{Eh^2 a_i} - \frac{(\beta_i + \mu)m^2\pi^2}{a_i b^2}\right)\frac{\mathrm{d}A_{im}}{\mathrm{d}\bar{x}_i} = 0,$$
$$i = 1,2 \tag{22b}$$

and the continuity equations at the separation interface are

$$\bar{w}_1\Big|_{\bar{x}_1=1} - \bar{w}_2\Big|_{\bar{x}_2=0} = 0 \Rightarrow A_{1m}|_{\bar{x}_1=1} - A_{2m}|_{\bar{x}_2=0} = 0, \tag{23a}$$

$$\frac{1}{a_1}\frac{\partial \bar{w}_1}{\partial \bar{x}_1}\bigg|_{\bar{x}_1=1} - \frac{1}{a_2}\frac{\partial \bar{w}_2}{\partial \bar{x}_2}\bigg|_{\bar{x}_2=0} = 0 \Rightarrow \frac{1}{a_1}\frac{\mathrm{d}A_{1m}}{\mathrm{d}\bar{x}_1}\bigg|_{\bar{x}_1=1} - \frac{1}{a_2}\frac{\mathrm{d}A_{2m}}{\mathrm{d}\bar{x}_2}\bigg|_{\bar{x}_2=0} = 0, \tag{23b}$$

$$\left(\frac{\alpha_1}{a_1^2}\frac{\partial^2 \bar{w}_1}{\partial \bar{x}_1^2} + \frac{\beta_1 - \mu}{b^2}\frac{\partial^2 \bar{w}_1}{\partial \bar{y}_1^2}\right)\bigg|_{\bar{x}_1=1} - \left(\frac{\alpha_2}{a_2^2}\frac{\partial^2 \bar{w}_2}{\partial \bar{x}_2^2} + \frac{\beta_2 - \mu}{b^2}\frac{\partial^2 \bar{w}_2}{\partial \bar{y}_2^2}\right)\bigg|_{\bar{x}_2=0} = 0$$
$$\Rightarrow \left(\frac{\alpha_1}{a_1^2}\frac{\mathrm{d}^2 A_{1m}}{\mathrm{d}\bar{x}_1^2} - \frac{m^2\pi^2(\beta_1 - \mu)}{b^2}A_{1m}\right)\bigg|_{\bar{x}_1=1} - \left(\frac{\alpha_2}{a_2^2}\frac{\mathrm{d}^2 A_{2m}}{\mathrm{d}\bar{x}_2^2} - \frac{m^2\pi^2(\beta_2 - \mu)}{b^2}A_{2m}\right)\bigg|_{\bar{x}_2=0} = 0, \tag{23c}$$

$$\left(\frac{\alpha_1}{a_1^3}\frac{\partial^3\bar{w}_1}{\partial\bar{x}_1^3}+\frac{(\beta_1+\mu)}{a_1b^2}\frac{\partial^3\bar{w}_1}{\partial\bar{x}_1\partial\bar{y}_1^2}+\frac{12\sigma_1 b}{Eh^2a_1}\frac{\partial\bar{w}_1}{\partial\bar{x}_1}\right)\Bigg|_{\bar{x}_1=1}-\left(\frac{\alpha_2}{a_2^3}\frac{\partial^3\bar{w}_2}{\partial\bar{x}_2^3}+\frac{(\beta_2+\mu)}{a_2b^2}\frac{\partial^3\bar{w}_2}{\partial\bar{x}_2\partial\bar{y}_2^2}+\frac{12\sigma_2 b}{Eh^2a_2}\frac{\partial\bar{w}_2}{\partial\bar{x}_2}\right)\Bigg|_{\bar{x}_2=0}=0$$

$$\Rightarrow\left[\frac{\alpha_1}{a_1^3}\frac{\mathrm{d}^3A_{1m}}{\mathrm{d}\bar{x}_1^3}+\left(\frac{12\sigma_1 b}{Eh^2a_1}-\frac{m^2\pi^2(\beta_1+\mu)}{a_1b^2}\right)\frac{\mathrm{d}A_{1m}}{\mathrm{d}\bar{x}_1}\right]_{\bar{x}_1=1}$$

$$-\left[\frac{\alpha_2}{a_2^3}\frac{\mathrm{d}^3A_{2m}}{\mathrm{d}\bar{x}_2^3}+\left(\frac{12\sigma_2 b}{Eh^2a_2}-\frac{m^2\pi^2(\beta_2+\mu)}{a_2b^2}\right)\frac{\mathrm{d}A_{2m}}{\mathrm{d}\bar{x}_2}\right]_{\bar{x}_2=0}=0. \tag{23d}$$

By substituting the appropriate solutions expressed in Eqs. (12)–(19) into Eqs. (20) to (23), one obtains a set of homogeneous equations which may be expressed in the following matrix form:

$$[K]\{C\}=\{0\} \tag{24}$$

in which $\{C\}=\{C_{11}\ C_{12}\ C_{13}\ C_{14}\ C_{21}\ C_{22}\ C_{23}\ C_{24}\}^{\mathrm{T}}$. For a nontrivial buckling solution, the determinant of $[K]$ must vanish. The characteristic equation furnishes the stability criterion. The valid solution combinations should satisfy the following requirements:

- The buckling load satisfies the limits of validity for the solution combinations which it belongs to.
- The buckling load is the lowest value among possible solutions and it was found that $m=1$ gives the lowest load for all possible m values for the considered cases.
- The stability curves are continuous.

3. Results and discussion

In order to examine the plastic buckling criteria of rectangular plates, we have adopted the following material properties: $E=10700$ ksi, $\sigma_0=61.4$ ksi, $v=0.32$ and the Ramberg–Osgood parameters $c=20$ and $k=0.3485$. The influences of material properties including E/σ_0 and c will also be investigated. The buckling factors for the end and intermediate loads are expressed as $\Lambda_1=\sigma_1 hb^2/(\pi^2 D)$ and $\Lambda_2=\sigma_2 hb^2/(\pi^2 D)$, respectively where $D=Eh^3/[12(1-v^2)]$ denotes the flexural rigidity of the plate.

Table 2 presents the plastic buckling stress for a simply supported, square plate under a uniaxial compressive end load. The results are compared with those obtained by Wang et al. (2001). It is observed that both results are in close agreement. Note that the results from Wang et al. (2001) are based on the Mindlin shear deformable plate theory. As expected, the results from Wang et al. (2001) are slightly smaller than the present results which are based on the classical thin plate theory.

Table 2
Plastic buckling stresses σ_1 for a simply supported, square plate under uniaxial end load (i.e. no intermediate load)

b/h	Buckling stresses σ_1 (in ksi)			
	IT		DT	
	Present study	Wang et al. (2001)	Present study	Wang et al. (2001)
22	71.61	70.84	61.90	60.08
24	61.15	60.71	58.54	57.40
26	54.88	54.60	54.39	53.81
28	49.41	49.11	49.32	48.96

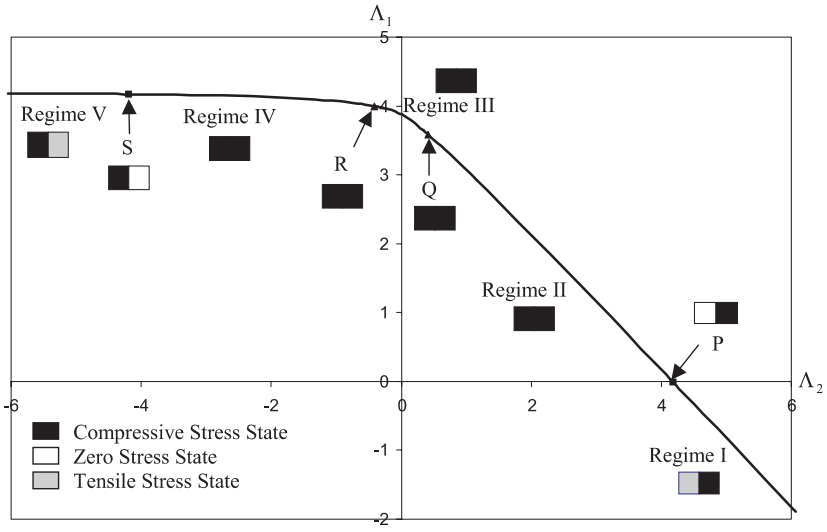

Fig. 3. Typical stability criterion curve for CSCS square plate with $h/b = 0.04$ by DT. The intermediate load is placed at $\eta = 0.5$.

Fig. 3 presents a typical stability criterion curve for plates subjected to intermediate and end loads. The negative values of Λ_i, $i = 1, 2$ denote tensile inplane loads. The plate will not buckle for any combination of Λ_1 and Λ_2 values which fall below the stability criterion curve.

The stability criterion curve consists of various regimes. For example, considering the case of a CSCS square plate with a thickness to width ratio $h/b = 0.04$ and subjected to an intermediate load located at $\eta = 0.5$, there are five regimes I, II, III, IV and V which are defined by solution combinations B + A, H + A, A + A, A + H and A + B, respectively (see Fig. 3). The critical points P, Q, R and S that connect the regimes are defined by the solution combinations G + A, F + A, A + F and A + G, respectively. Point P represents the loading case in which the inplane load is applied to sub-plate 2 only (i.e. $N_1 = 0$) whereas point S represents the loading case where only sub-plate 1 is loaded (i.e. $N_1 + N_2 = 0$). However, for different material properties, aspect ratios, intermediate load positions, and boundary conditions the solution combinations may change somewhat.

3.1. Buckling factors with various aspect ratios a/b

Figs. 4–6 show the stability criterion curves of SSSS, CSCS and FSFS rectangular plates with aspect ratios $a/b = 1.0$, 2.0 and 3.0, the intermediate loading position $\eta = 0.5$, thickness to width ratio $h/b = 0.04$ and various end load to intermediate load ratios. Figs. 4a, 5a and 6a show the buckling results using IT while Figs. 4b, 5b and 6b present results using DT. The two plasticity theories furnish somewhat similar results except for the case of CSCS square plates.

Referring to Figs. 4 and 5, we can see that for SSSS and CSCS plates, the buckling factors decrease with the increasing aspect ratios a/b. However, for FSFS plates, the buckling factors with $a/b = 1.0$ could be smaller than that of $a/b = 2.0$ and $a/b = 3.0$ as shown in Fig. 6. For SSSS and CSCS plates, the differences between the buckling factors for $a/b = 2.0$ and $a/b = 3.0$ are however much smaller than the differences between those for $a/b = 1.0$ and $a/b = 2.0$.

For negative values of the intermediate load factor Λ_2 (i.e. Λ_2 is tensile in nature), the end buckling factor Λ_1 takes on almost a constant value. This is because sub-plate 2 does not buckle as it is under a very

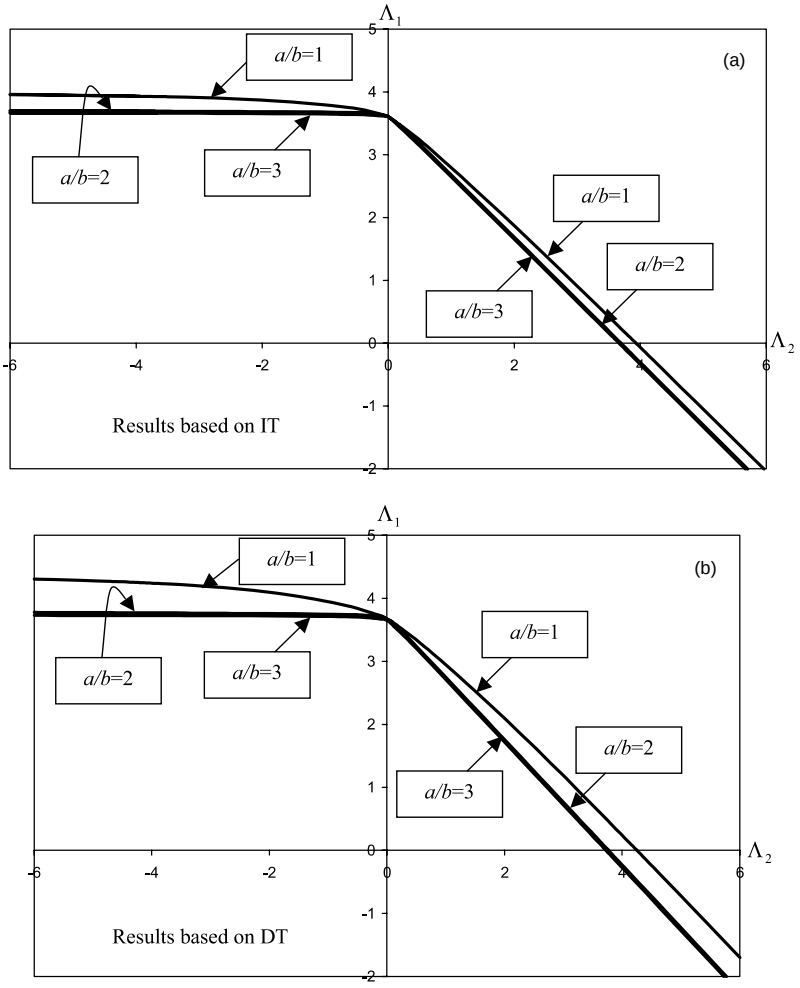

Fig. 4. Stability criteria for SSSS rectangular plates with $h/b = 0.04$ and different aspect ratios $a/b = 1, 2, 3$ by (a) IT and (b) DT. The intermediate load is placed at $\eta = 0.5$.

low compressive stress state or in a tensile stress state. So the buckling deformation of the plate mainly occurs in sub-plate 1. In order to reinforce this point, consider a rectangular plate with two opposite edges simply supported, subject to an end load and an intermediate load located at $\eta = 0.5$, as shown in Fig. 7a. Suppose we let sub-plate 2 be subjected to a large tensile stress state, say $\Lambda_2 = -50$. Depending on different boundary conditions of the other two edges, the buckling factors Λ_1 are given in Table 3. We now compare the buckling stresses of rectangular plates whose aspect ratio $a/b = 0.5$ and having the same boundary conditions as sub-plate 1 along three edges, as shown in Fig. 7b, but the X edge may be clamped, simply-supported or free edge. The corresponding buckling factors are given in Table 3 for comparison. Based on the results presented in Table 3 for SSSS, CSCS and FSFS plates, we can conclude that when sub-plate 2 is under a large tensile stress state, the interface edge may be regarded as approaching the condition of a clamped edge, except for the FSFS plate with $a/b = 2.0$, where the interface edge imposes a constraint to the plate similar to the one from a simply-supported edge.

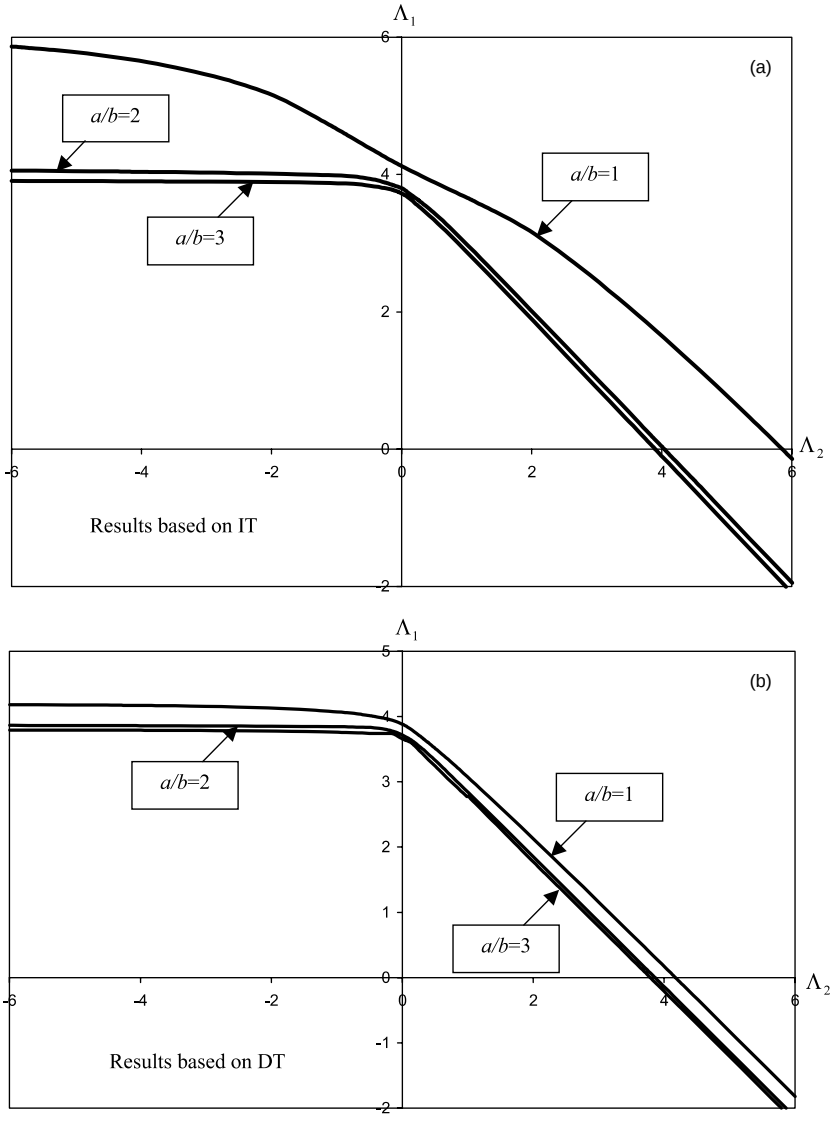

Fig. 5. Stability criteria for CSCS rectangular plates with $h/b = 0.04$ and different aspect ratios $a/b = 1, 2, 3$ by (a) IT and (b) DT. The intermediate load is placed at $\eta = 0.5$.

3.2. Buckling factors with various loading positions η

Based on IT and DT, Fig. 8a and b shows the variations of the buckling factors Λ_2 of SSSS rectangular plates with respect to loading positions η when $\Lambda_1 = 0, 2$, $a/b = 1, 2$, and thickness to width ratio $h/b = 0.04$ respectively. It can be seen that the buckling factor Λ_2 increases with the increasing value of η, albeit gradually for $\eta < 0.7$ and more steeply for $\eta \geqslant 0.7$. It can be seen that the two theories of plasticity furnish significantly different buckling values when $\eta \geqslant 0.7$, especially for results based on IT. Generally, buckling factors associated with IT are higher than their DT counterparts. It is worth noting that the buckling factors Λ_2 for $\Lambda_1 = 0$ differ from their counterparts associated with $\Lambda_1 = 2$ by an approximate factor of 2.

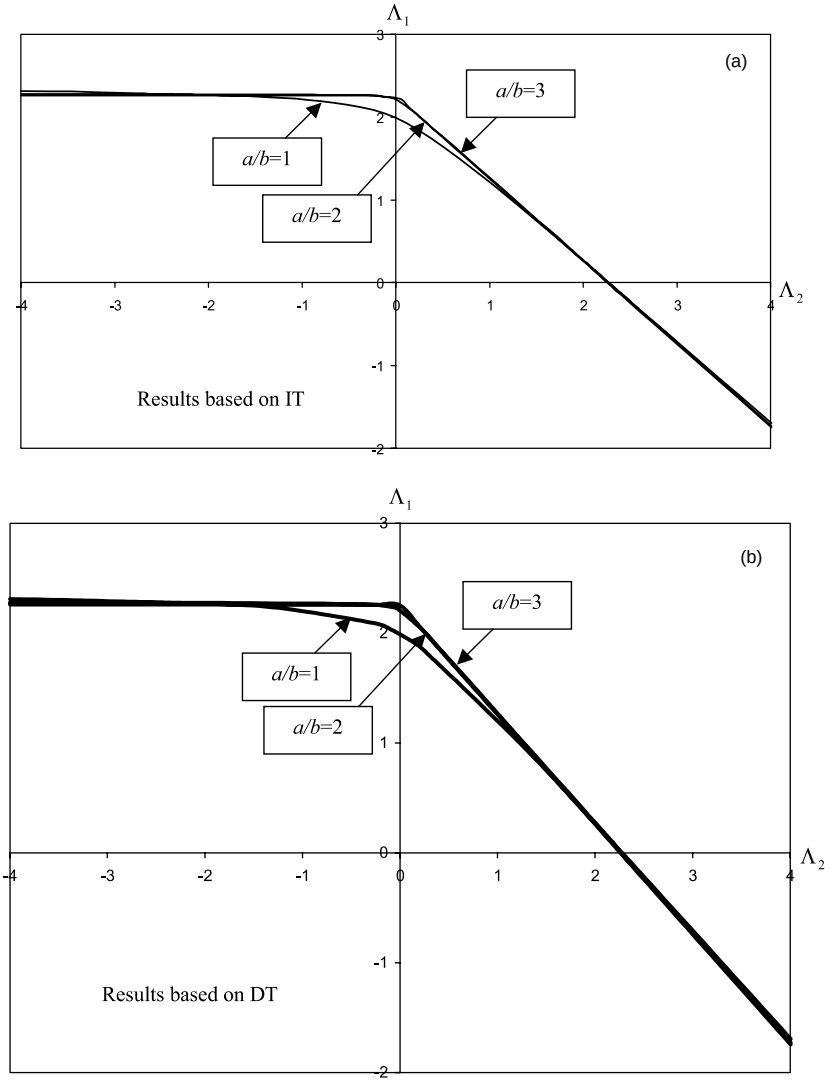

Fig. 6. Stability criteria for FSFS rectangular plates with $h/b = 0.04$ and different aspect ratios $a/b = 1, 2, 3$ by (a) IT and (b) DT. The intermediate load is placed at $\eta = 0.5$.

3.3. Buckling factors with various boundary conditions

The influences of boundary conditions (such as SSSS, CSCS, FSFS, CSSS, FSSS and CSFS) on the buckling factors are highlighted in Fig. 9. In computing these buckling factors, we have used the following parameters: aspect ratio $a/b = 2.0$, thickness to width ratio $h/b = 0.04$ and intermediate load position $\eta = 0.5$. It can be seen from Fig. 9 that the buckling criterion curves merge at some portions even though the rectangular plates have one of its edge conditions different from the other provided the sub-plate with this edge is under a high tensile stress state. For example, a CSFS plate with a high tensile stress state in sub-plate 2 will behave in a similar manner to a CSCS plate with a high tensile stress state or a low compressive

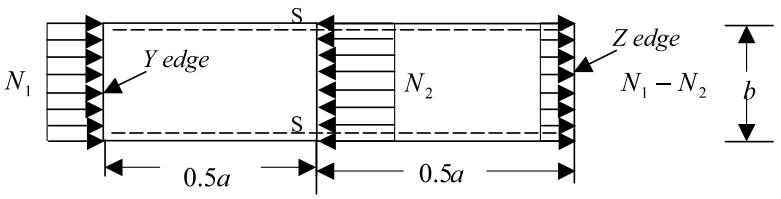

(a) Full plate *YSZS*

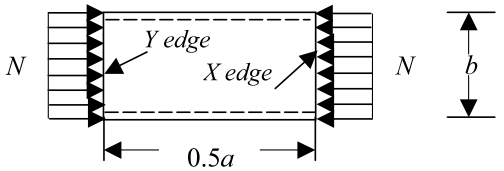

(b) Sub-plate *YSXS*

Fig. 7. Rectangular plate YSZS and corresponding sub-plate YSXS under uniaxial load.

Table 3
Comparison of buckling factors of full plates with uniaxial intermediate and end loads and their corresponding end loaded sub-plates with different interfacial edge conditions

	IT	DT	IT	DT	IT	DT
Buckling factor Λ_1 for SSSS with $\Lambda_2 = -50$	$a/b = 1.0$		$a/b = 2.0$		$a/b = 3.0$	
	4.470	4.002	3.799	3.712	3.738	3.674
Buckling factors for SSXS sub-plate	$a/b = 0.5$		$a/b = 1.0$		$a/b = 1.5$	
X edge is clamped	4.543	4.015	3.806	3.717	3.742	3.679
X edge is simply-supported	3.893	3.797	3.678	3.605	3.631	3.609
X edge is free	1.990	1.990	2.311	2.311	2.253	2.253
Buckling factor Λ_1 for CSCS with $\Lambda_2 = -50$	$a/b = 1.0$		$a/b = 2.0$		$a/b = 3.0$	
	6.214	4.198	4.108	3.878	3.917	3.802
Buckling factors for CSXS sub-plate	$a/b = 0.5$		$a/b = 1.0$		$a/b = 1.5$	
X edge is clamped	6.367	4.205	4.123	3.884	3.924	3.806
X edge is simply-supported	4.543	4.015	3.806	3.717	3.742	3.679
X edge is free	2.568	2.568	2.333	2.333	2.270	2.270
Buckling factor Λ_1 for FSFS with $\Lambda_2 = -50$	$a/b = 1.0$		$a/b = 2.0$		$a/b = 3.0$	
	2.451	2.451	2.289	2.289	2.266	2.266
Buckling factors for FSXS sub-plate	$a/b = 0.5$		$a/b = 1.0$		$a/b = 1.5$	
X edge is clamped	2.568	2.568	2.333	2.333	2.270	2.270
X edge is simply-supported	1.990	1.990	2.311	2.311	2.253	2.253
X edge is free	1.539	1.539	1.990	1.990	2.210	2.210

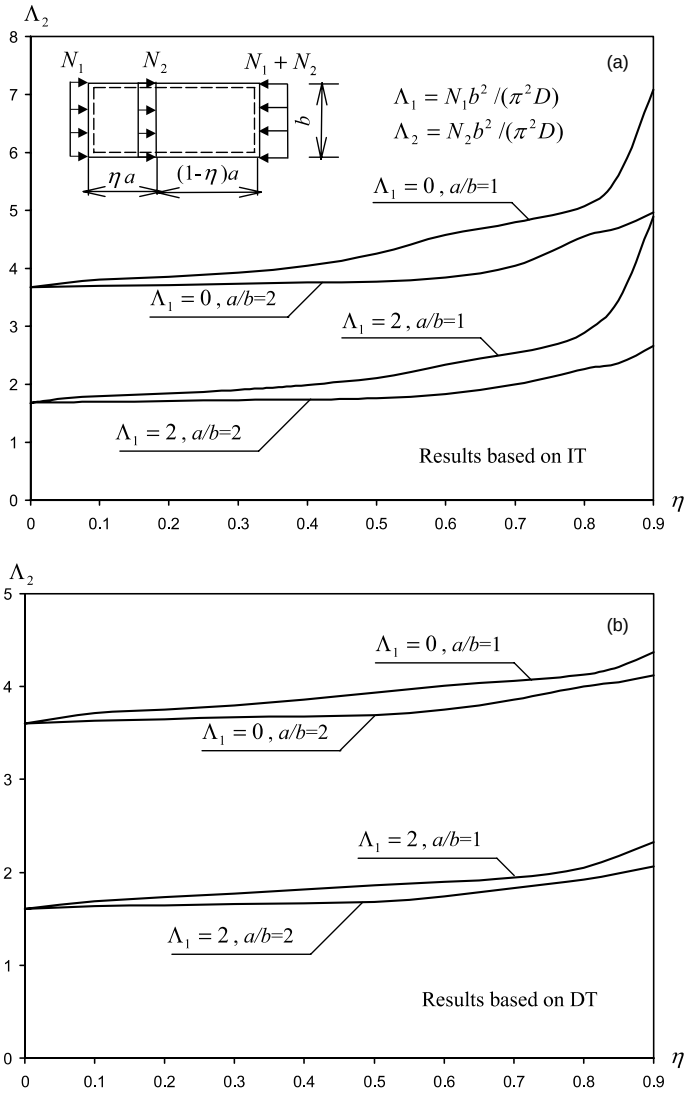

Fig. 8. Variation of buckling factors Λ_2 with respect to η for rectangular plates with $\Lambda = 0$ and 2 by (a) IT and (b) DT.

stress state in sub-plate 2 because the tensile stressed sub-plate does not buckle at all and thus its edge condition plays no part in the buckling phenomenon.

3.4. Buckling factors with various material properties

The buckling factors of SSSS square plates with various material properties $E/\sigma_0 = 200$, 400, 800 and $c = 2$, 3, 20 are given in Figs. 10 and 11 by using IT and DT, respectively. A thickness to width ratio $h/b = 0.04$, and loading position $\eta = 0.5$ were used in the calculations. It can be seen from Figs. 10 and 11 that the buckling factors decrease with increasing values of hardening index c, i.e. as the plate material approaches the perfectly elastic–plastic constitutive relation. Furthermore, the shape of the stability cri-

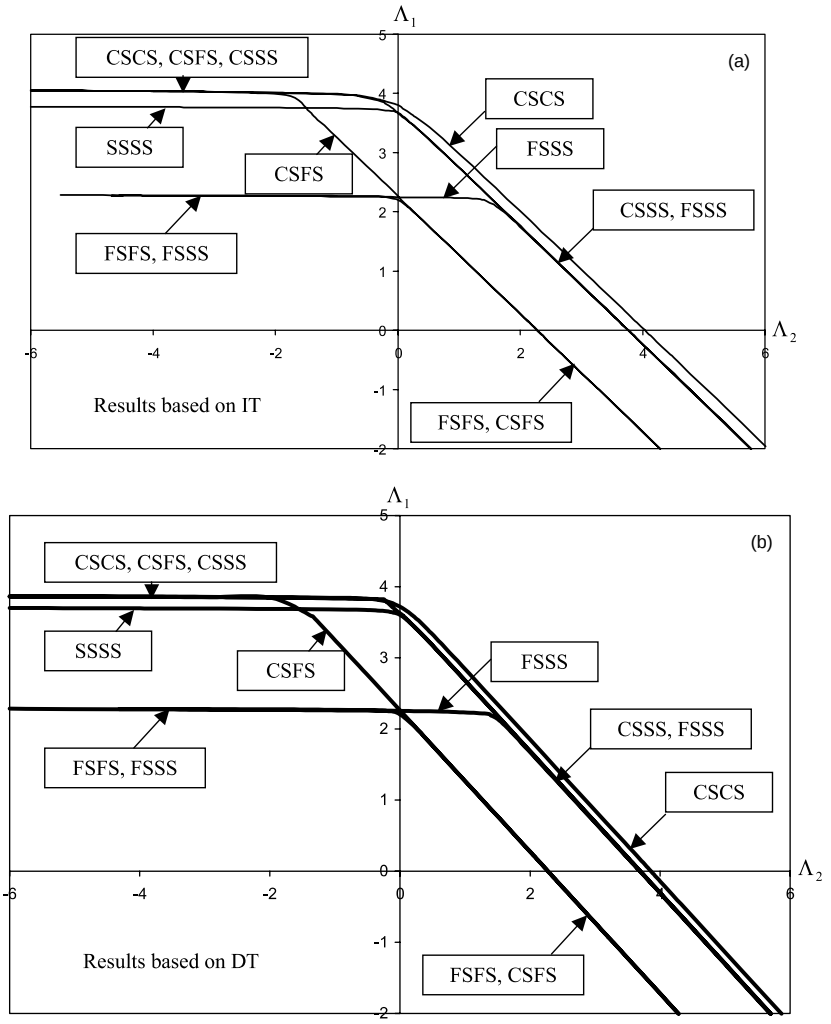

Fig. 9. Stability criteria for rectangular plates with $h/b = 0.04$, aspect ratio $a/b = 2$, intermediate load position $\eta = 0.5$ and different boundary conditions by (a) IT and (b) DT.

terion curve for large c values approach a bilinear curve with a horizontal portion when Λ_2 is negative and a linear curve when Λ_2 is positive. The slope of the linear portion is given by Λ_1^*/Λ_2^* where Λ_1^* is Λ_1 value when $\Lambda_2 = 0$ (i.e. the case when the plate is subjected to only end load) and Λ_2^* is Λ_2 value when $\Lambda_1 = 0$ (i.e. the case when the plate is subjected to only intermediate load).

3.5. Buckling factors from two theories

The buckling factors of SSSS square plates with various material properties $E/\sigma_0 = 200$, 400, 800 and under an intermediate load only are given in Fig. 12 by using IT and DT, respectively. From Fig. 12, we observe that the difference between IT and DT increases with increasing E/σ_0 values. For the same value of E/σ_0, the differences also increases with increasing values of parameter c.

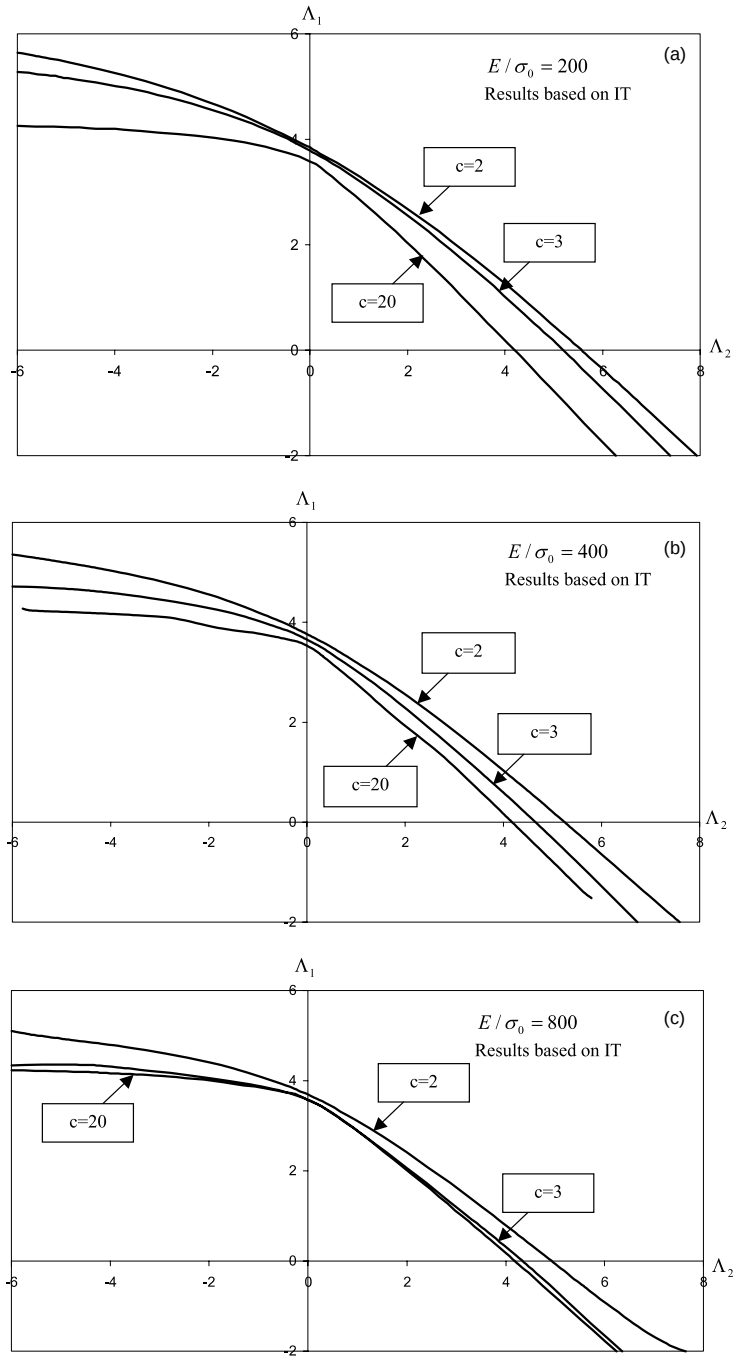

Fig. 10. Stability criteria for SSSS square plates with $h/b = 0.04$, $\eta = 0.5$, for different $\frac{E}{\sigma_0}$ = (a) 200, (b) 400, (c) 800 by IT.

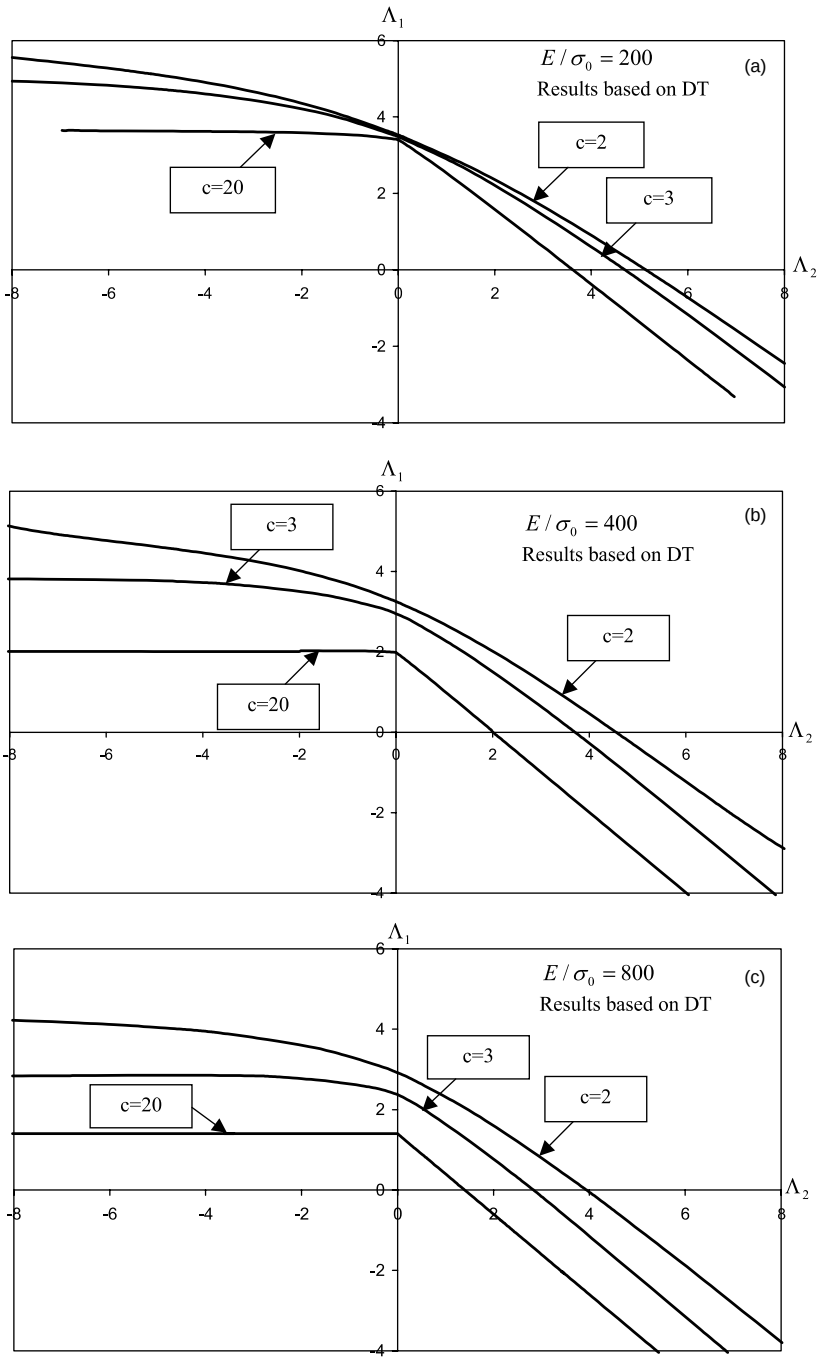

Fig. 11. Stability criteria for SSSS square plates with $h/b = 0.04$, $\eta = 0.5$, for different $\frac{E}{\sigma_0}$ = (a) 200, (b) 400, (c) 800 by DT.

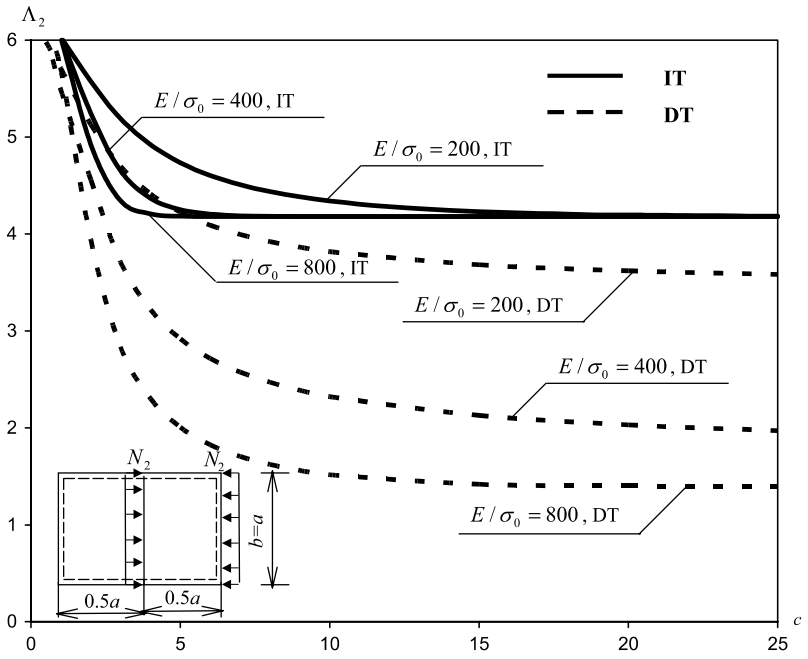

Fig. 12. Buckling load factors Λ_2 for SSSS square plates with $\Lambda_1 = 0$.

4. Conclusions

This paper presents an analytical method for determining the exact plastic buckling factors of rectangular plates subjected to end and intermediate uniaxial loads, and where two opposite edges (parallel to the loads) of the plates are simply supported. In this method, the rectangular plate is divided into two sub-plates at the intermediate load location. Each sub-plate buckling problem is then solved using the Levy approach. There are eight feasible solutions for each sub-plate. The critical buckling load is determined from one of the 64 possible solution combinations for the two sub-plates. The solution combination depends on the aspect ratio, the intermediate load position, the intermediate to end load ratio, the material properties and the boundary conditions. The effects of the aforementioned parameters and the adoption of DT and IT on the buckling factors are also investigated.

The presented exact buckling solutions do not only elucidate the intrinsic and fundamental characteristics of the buckling solutions but they should be useful to researchers as benchmark values for checking the convergence, validity and accuracy of numerical methods for plate buckling analysis.

References

Betten, J., Shin, C.H., 2000. Elastic–plastic buckling analysis of rectangular plates subjected to biaxial loads. Forschung Im Ingenieurwesen—Engrg. Res. 65 (9), 273–278.

Bijlaard, P.P., 1949. Theory and tests on the plastic stability of plates and shells. J. Aero. Sci. 16, 529.

Bulson, P.S., 1970. The Stability of Flat Plates. Chatto and Windus, London, UK.

Chakrabarty, J., 2000. Applied Plasticity. Springer-Verlag, Berlin.

Chakrabarty, J., 2002. Influence of anisotropy on the plastic buckling of rectangular plates. In: C.M. Wang, G.R. Liu, K.K. Ang (Eds.), Proc. of 2nd Int. Conf. Struct. Stability and Dynamics, World Scientific, Singapore, December 16–18, pp. 448–452.

Durban, D., 1998. Plastic buckling of plates and shells. Stability analysis of plates and shells. NACA/CP-1998-206280, p. 293.
Durban, D., Zuckerman, Z., 1999. Elastoplastic buckling of rectangular plates in biaxial compression/tension. Int. J. Mech. Sci. 41, 751–765.
El-Ghazaly, H.A., Sherbourne, A.N., 1986. Deformation theory for elastic–plastic buckling analysis of plates under non-proportional planar loading. Comput. Struct. 22 (2), 131–149.
Handelman, G.H., Prager, W., 1948. Plastic buckling of a rectangular plate under edge thrusts. NACA Technical Note No. 1530, Washington, USA.
Hencky, H., 1925. Uber langsame stationare stromungen in plastischen massen mit rucksicht auf die vorgange beim walzen. Pressen und Ziehen von Metallen. Z.f.a.M.M., Bd. 5, Heft 2, 115.
Hutchinson, J.W., 1974. Plastic buckling. Adv. Appl. Mech. 14, 67.
Ilyushin, A.A., 1946. The elasto-plastic stability of plates. NACA Technical Memorandum no. 1188, Washington, USA.
Moen, L.A., Langseth, M., Hopperstad, O.S., 1998. Elastoplastic buckling of anisotropic aluminium plate elements. J. Struct. Engrg. ASCE 124 (6), 712–719.
Nadai, A., 1944. Plasticity. McGraw-Hill, New York.
Ore, E., Durban, D., 1992. Elastoplastic buckling of axially compressed circular cylindrical shells. Int. J. Mech. Sci. 34 (9), 727–742.
Prager, W., 1938. On isotropic materials with continuous transition from elastic to plastic state. In: Proc. Fifth Int. Cong. Appl. Mech. Cambridge, Massachusetts, USA.
Prager, W., 1941. A new mathematical theory of plasticity. Prikl. Mat. i Mekh. Moscow 5 (3), 419–427.
Prager, W., 1942a. Fundamental theorems of a new mathematical theory of plasticity. Duke Math. J. 9 (1), 228–233.
Prager, W., 1942. Theory of plasticity. Brown Univ. Mimeographed Lecture Notes. Providence, RI (Chapter VII).
Pride, R.A., Heimerl, G.J., 1949. Plastic buckling of simply supported compressed plates. NACA Technical Note No. 1817, Washington, USA.
Sewell, M.J., 1963. A general theory of elastic and inelastic plate failure, Part 1. J. Mech. Phys. Solids 11, 377.
Shanley, F.R., 1946. Inelastic column theory. J. Aero. Sci. 14, 261–268.
Shrivastava, S.C., 1979. Inelastic analysis of plates including shear effects. Int. J. Solids Struct. 15, 567–575.
Shrivastava, S.C., 1995. Inelastic buckling of rectangular sandwich plates. Int. J. Solids Struct. 32 (8–9), 1099–1120.
Soh, A.K., Bian, L.C., Chakrabarty, J., 2000. Elastic/plastic buckling of a composite flat plate subjected to uniform edge compression. Thin-Walled Struct. 38 (3), 247–265.
Stowell, E.Z., 1948. A unified theory of plastic buckling of columns and plates. NACA Technical Note No. 1556, Washington, USA.
Timoshenko, S.P., Gere, J.M., 1961. Theory of Elastic Stability. McGraw-Hill, New York.
Timoshenko, S.P., Woinowsky-Krieger, S., 1959. Theory of Plates and Shells. McGraw-Hill, New York.
Wang, C.M., Xiang, Y., Chakrabarty, J., 2001. Elastic/plastic buckling of thick plates. Int. J. Solids Struct. 38, 8617–8640.
Wang, C.M., Chen, Y., Xiang, Y., 2004. Stability criteria for rectangular plates subjected to intermediate and end inplane loads. Thin-Walled Struct. 42, 119–136.
Wang, C.M., 2004. Plastic buckling of simply supported, polygonal Mindlin plates. J. Engrg. Mech., ASCE 130 (1), 117–122.
Xiang, Y., Wang, C.M., Kitipornchai, S., 2003. Exact buckling solutions for rectangular plates under intermediate and end uniaxial loads. J. Engrg. Mech., ASCE 129, 835–838.